Assessing surface heat flux products with *in situ* observations over the Australian sector of the Southern Ocean

Vidhi Bharti[1,2], Eric Schulz[3], Christopher W. Fairall[4], Byron W. Blomquist[4], Yi Huang[1,2], Alain Protat[3], Steven T. Siems[1,2], Michael J. Manton[1]

[1]School of Earth, Atmosphere and Environment, Monash University, Victoria, Australia

[2]Australian Research Council Centre of Excellence for Climate System Science, Monash University, Victoria, Australia

[3]Australian Bureau of Meteorology, Melbourne, Victoria, Australia

[4]National Oceanic and Atmospheric Association, Earth Systems Research Laboratory, Boulder, CO, USA

Abstract

Given the large uncertainties in surface heat fluxes over the Southern Ocean, an assessment of fluxes obtained by European Centre for Medium-Range Weather Forecasts (ECMWF) interim reanalysis product (ERA-Interim), the Australian Integrated Marine Observing System (IMOS) routine observations and Objectively Analyzed air-sea heat Fluxes (OAFlux) project hybrid dataset is performed. The surface fluxes are calculated using COARE 3.5 bulk algorithm using *in-situ* data obtained from the NOAA PSD flux system during the *CAPRICORN* experiment onboard *R/V Investigator* voyage (March-April 2016) in the Australian sector of the Southern Ocean (43°S to 53°S). ERA-Interim and OAFlux data are further compared with the Southern Ocean Flux station (SOFS) air-sea flux moored surface float deployed for a year (March 2015 – April 2016) at ~46.7°S, 142°E. The results indicate that ERA-Interim (3-hourly at 0.25°) and OAFlux (daily at 1°) estimate sensible heat flux, H_s accurate to within ±5 Wm^{-2} and latent heat flux, H_l to within ±10 Wm^{-2}. ERA-Interim gives a positive bias in H_s at low latitudes (<47°S) and in H_l at high latitudes (>47°S), and OAFlux displays consistently positive bias in H_l at all latitudes. No systematic bias with respect to wind or rain conditions was observed. Although some differences in the bulk flux algorithms are noted, these biases can be largely attributed to the uncertainties in the observations used to derive the flux products.

1. Introduction

The poor knowledge of surface heat fluxes over the Southern Ocean contributes to large uncertainty in the global surface heat and ocean heat budget closure (Josey et al. 1999;

Fasullo and Trenberth 2008). The current goal set by global climate community is to achieve global surface net flux accuracy of ±10 Wm^{-2} at a monthly resolution (Fairall et al. 2010), which implies determining fluxes accurately to within 5 Wm^{-2} at 3-6 hour time resolution and 1° spatial resolution (Curry et al. 2004). Several global satellite-derived flux products have been released in the past, however, substantial disagreement among them has been reported over the Southern Ocean. The satellite products capture the spatiotemporal patterns accompanied with large variances (15-25 Wm^{-2}) and substantial differences in the spatiotemporal distribution of fluxes [annual mean for latent heat flux (H_l) 54-69 Wm^{-2} and -0.2 – 21 Wm^{-2} for sensible heat flux (H_s)] (Liu et al. 2011; Yu et al. 2011). Further, reanalysis products perform poorly with biases reported as high as 100 Wm^{-2} on any given day over the Southern Ocean (Dong et al. 2007). Calibration uncertainties in satellite instruments, regional biases in bulk variables, inconsistencies in transfer coefficients of bulk algorithms and large sampling errors due to unique conditions have been cited as potential sources of errors. The large biases in the energy budget of the southern hemisphere in reanalysis products have also been linked to a poor simulation of clouds (Trenberth and Fasullo 2010). Further, the impact of mesoscale oceanic eddies on the surface heat budget is yet to be fully resolved over the Southern Ocean (Bôas et al. 2015; Frenger et al. 2013). The acquisition of additional high-quality *in situ* observations via implementation of moorings and voluntary observing ships (VOS), and inter-comparison of flux products for the improvement of surface flux estimates over high latitude oceans has been recommended (Bourassa et al. 2013; Gille et al. 2010). There is a serious dearth of *in situ* observations over the Southern Ocean region due to its remote location and challenging environment. The region poses severe logistical challenges; hence, conducting frequently dedicated experiments using sensitive instruments employed for flux measurements onboard research vessels is an expensive and challenging task. Therefore, the *in-situ* data obtained during these occasional experiments must be employed to reduce biases in routine ship observations which act as inputs to satellite and reanalyses products.

Two flux products available over the Southern Ocean - the combined satellite-reanalyses dataset, Objectively Analyzed air-sea Heat Fluxes (OAFlux) project at the Woods Hole Oceanographic Institution (Yu *et al.*, 2008) and the European Centre for Medium-Range Weather Forecasts (ECMWF) interim reanalysis (ERA-Interim) flux estimates (Dee et al. 2011) have previously been examined for global oceans (Herman 2015). The OAFlux is reported to be in reasonable agreement with ship-based climatology and buoys (5% average) due to improved estimations of flux-related input variables over global oceans (Jiang et al. 2012; Yu et al. 2004, 2007; Yu and Weller 2007). Previous studies have identified the smallest biases in ERA-Interim heat flux estimates out of several reanalyses products when compared with

69 the observations (Balsamo et al. 2015; Decker et al. 2012; Lindsay et al. 2014; Szczypta et al.
70 2011). However, the performance of ERA-Interim and OAFlux could not be fully assessed over
71 the Southern Ocean owing to the absence of any ground reference data set.

72 The *Clouds, Aerosols, Precipitation, Radiation, and atmospherIc Composition Over the*
73 *southeRn oceaN* (hereafter CAPRICORN) phase 1 experiment was carried out during 14 March
74 - 15 April 2016 in the Australian sector of the Southern Ocean undertaken by the *R/V*
75 *Investigator*. The primary objectives were to study clouds, precipitation, atmospheric
76 composition, surface energy budget and biogeochemistry in the Southern Ocean. The voyage
77 sampled one cyclonic eddy (cold core) for 6 days and one anticyclonic (warm core) eddy for
78 4 days in the Antarctic Circumpolar Current and encountered several extratropical cyclones.
79 One of the principal aims of the project was to acquire high-quality direct flux observations
80 using the National Oceanic and Atmospheric Administration Physical Sciences Division (NOAA
81 PSD) flux system to validate those derived by the bulk aerodynamic approach, as well as
82 satellite-based and reanalysis products. The bulk fluxes were calculated by the Coupled
83 Ocean-Atmosphere Response Experiment (COARE) bulk algorithm (Fairall et al. 1996b), a
84 state-of-the-art approach for calculating turbulent fluxes over the open oceans in recent
85 years. Although initially developed for the tropical oceans, the model has been progressively
86 revised for varying wind-wave conditions in the tropics and mid-latitude oceans (Brunke et
87 al. 2003; Edson et al. 2013; Fairall et al. 2003).

88 Additionally, a large moored surface float, the Southern Ocean Flux Station (SOFS), has been
89 deployed since 2010 as part of the Australian Integrated Marine Observing System (IMOS)
90 Southern Ocean Time Series (SOTS) project which has been used to study fluxes in the
91 Southern Ocean previously (Schulz et al. 2011, 2012). A 13-month deployment covering
92 March 2015 to April 2016 is used in this study.

93 The objective of the current study is to evaluate the accuracy of flux products on a variable
94 spatiotemporal scale over the Australian sector of the Southern Ocean against the high-
95 quality *in situ* observations. It is to be noted that ERA-Interim and OAFlux products are
96 gridded flux products, therefore, these flux values are averaged over the grid containing the
97 *in situ* point measurements. Whilst we acknowledge this disparity between spatiotemporal
98 resolutions of studied flux products, albeit, it should not lead to atypical results. An evaluation
99 of the physical processes that underpin the observed flux characteristics is being addressed
100 in a separate study (Bharti *et al.*, 2018, submitted to JGR). Thus, this paper compares the
101 surface sensible (H_s) and latent heat fluxes (H_l) (radiative fluxes not included) obtained from
102 the CAPRICORN experiment and moored surface float with those estimated by OAFlux, ERA-

Interim and the routine *R/V Investigator* ship observations collected using standard instruments as part of IMOS.

2. Bulk parameterization algorithms

All the bulk parameterization algorithms are based on the Monin - Obukhov similarity theory (MOST), with the turbulent fluxes given by:

$$\tau = \rho C_D (U_{10} - U_0)|U_{10} - U_0| \quad (1)$$

$$H_s = \rho c_p C_H (\theta_{10} - \theta_0)|U_{10} - U_0| \quad (2)$$

$$H_l = \rho L_v C_E (q_{10} - q_0)|U_{10} - U_0| \quad (3)$$

where τ indicates wind stress, ρ and c_p are the density and isobaric specific heat of air respectively; L_v is the latent heat of vaporization; θ is the potential temperature; and transfer coefficients for momentum (drag coefficient), heat (Stanton number), and moisture (Dalton number) at 10-m height are C_D, C_H, and C_E respectively. The subscript '0' indicates the value at the interface; the subscript '10' indicates the 10-m height value.

In COARE 3.5, the transfer coefficients for heat and moisture are assumed the same. However, the transfer coefficients are derived from profile functions which in turn are affected by surface roughness, atmospheric stability, wind speed, sea state and precipitation. Since these transfer coefficients are still being improved over mid-latitudes and strong wind regimes, these bulk fluxes are not free from biases. Disagreement in the ship and buoy-based transfer coefficients has also been noted in previous studies (e.g., Edson, 2015). The input parameters have been progressively improved and corrected in the model. The details of the advent, progression and corrections in COARE bulk parameterization model are discussed in Fairall *et al.*, (2003), Bradley and Fairall, (2006) and Fairall *et al.*, (1996b).

3. Datasets

3.1 Surface observations

i) *R/V Investigator* 2016 cruise

The atmospheric and oceanic parameters were measured with the NOAA PSD flux system (turbulence variables sampled at 10 Hz and others at 1 Hz) onboard the ship. The voyage itself was one of its first efforts to conduct such an experiment in the Australian sector of the Southern Ocean. A cold eddy located at approximately 146.01°E, 50.37°S (dimensions roughly 141 x 111 km) and was sampled for 6 days starting from March 30, 2016, to April 5, 2016. A

warm eddy was also located as a part of a forming meander (roughly 123 km wide) and was sampled for approximately 4 days starting from April 6 to April 10, 2016. These eddies (figure 1) were identified using a spatial map of average global sea level anomalies. During the voyage, 9 extratropical cyclones were also encountered which caused sudden shifts in wind speed, wind direction, precipitation and sea-state conditions. The details of identification and description of cold front and warm sector are discussed in (Bharti et al. 2018) (submitted to JGR).

Although the cruise had to endure strong winds (up to 22 ms^{-1}) and sea conditions (wave-height up to 8 m), altogether the instruments functioned well resulting in a very high-quality observational dataset (Bariteau et al. 2018). However, ~48% of the flux values obtained by the direct eddy covariance system had to be discarded during preliminary quality control. The bulk fluxes were calculated using the COARE 3.5 bulk model and were compared with filtered direct flux values. Overall, the bulk flux values correlate well (>95%, p-value close to zero) with direct flux observations at hourly scale during the voyage (figure 2a and 2b). The detailed discussion on the direct and bulk fluxes during *R/V Investigator* 2016 voyage can be found in Bharti *et al*., (2018) [submitted to JGR]. Thus, COARE 3.5 bulk fluxes (hereafter referred to as CAPRICORN fluxes) are used as *in situ* observations for the validation of other flux products in the present paper. The CAPRICORN fluxes are converted to daily, 3-hourly and hourly fluxes to be compared with OAFlux, ERA-Interim and IMOS fluxes respectively.

ii) IMOS routine bulk fluxes

The IMOS gathered the routine ship observations during the *R/V Investigator* voyage alongside NOAA PSD flux observations. After the Bureau of Meteorology (BoM) quality control procedure, momentum and heat fluxes were calculated using the COARE 3.0 bulk model with these observations. There are significant gaps in the data, however, due to two reasons: first, the system failed to transmit observations from the ship to the shore from 14 March 2016 to 23 March 2016. Second, a large part of IMOS observations attributed to poor sampling conditions or instrument performance were omitted during preliminary quality control. Hence, usable data are available only from 24 March 2016 to 15 April 2016 (reconstructed to hourly estimates for comparison purpose). Overall, ~49% of the reconstructed hourly data remains missing. The data availability for IMOS *Investigator* data is shown in figure 1 with respect to the ship track.

iii) SOFS Buoy

The SOFS is the long-term air-sea flux moored surface float deployed intermittently since 2010 near 46.7°S 142°E (shown in figure 1) for the Integrated Marine Observing System

(IMOS). Here, we use SOFS data acquired over the period from March 2015 to April 2016. The buoy provides near real-time surface meteorological and ocean observations, and radiative components continuously at the 1-minute sampling rate. Momentum, heat and moisture fluxes are calculated using the COARE 3.5 bulk model after quality control has been applied.

3.2 Surface flux products

i) OAFlux

The OAFlux project provides heat fluxes for the global ice-free ocean basins. These heat fluxes are computed using the COARE 3.0 bulk flux algorithm following the construction of improved estimates of surface meteorological variables from a blending of satellite retrievals and three atmospheric reanalyses products – NCEP1, NCEP2 and ERA-40 (Yu et al. 2008). The satellite wind speed comes from three inputs – passive radiometers SSMI (Special Sensor Microwave Imager), AMSR-E (Advanced Microwave Scanning Radiometer-Earth Observing System) and QuikSCAT scatterometer. Near-surface humidity is derived from SSMI column water vapour retrievals (Chou et al. 2003) and height adjusted to 2-m based on the COARE 3.0 algorithm. SST data are derived from NOAA Optimum Interpolation (OI) (Reynolds et al. 2007). The third version of the OAFlux product, available for 32 years (1985-present) on daily time scale at 1° resolution grid, has been employed in the paper. The pixels are extracted based on the ship track and buoy location at daily scale for comparison with cruise and buoy respectively.

ii) ERA-Interim reanalysis product

The ERA-Interim reanalysis model estimates time-integrated surface sensible and latent heat fluxes as accumulated from the beginning of the forecast for every 3-hour window (Balsamo et al. 2015). For this study, the forecast fluxes are obtained for every 3-hour with initial conditions starting from 00Z at 0.25° resolution. For comparison with cruise and buoy data, grids are extracted relative to the ship track and buoy location respectively. The surface heat fluxes are computed using a first order K-diffusion closure in the surface layer and are calculated based on the bulk formulation where the transfer coefficients are estimated in terms of profile functions in accordance with the MOST (Beljaars 1998; ECMWF 2015a).

4. Results

4.1 Assessment of IMOS routine fluxes with ship fluxes

The IMOS routine fluxes are compared with the CAPRICORN fluxes. Despite large gaps, IMOS estimates give strong positive correlation (~0.9 at p~0) with CAPRICORN fluxes at hourly

scale. The mean H_s and H_l values for IMOS fluxes are 19.8 and 83.8 Wm^{-2} lying close to the CAPRICORN fluxes at 17.8 and 81.5 Wm^{-2} respectively as shown in table 1 and figure 2a and 2b. Further, it gives a lower mean error (2 Wm^{-2}) and RMSE (9 Wm^{-2}) for H_s values as compared to the same for H_l values.

IMOS fluxes are compared with CAPRICORN fluxes over the eddies. IMOS gives a positive bias of 1.73 Wm^{-2} in H_s and 1.97 Wm^{-2} in H_l over the warm eddy, but positive and small negative biases of 1.34 Wm^{-2} and -0.45 Wm^{-2} in H_s and H_l values respectively over the cold eddy. Overall, RMSE in H_s increases over eddies (11.60 Wm^{-2} over cold eddy and 9.27 Wm^{-2} over warm eddy) but decreases in H_l (17.52 Wm^{-2} over cold eddy and 15.10 Wm^{-2} over warm eddy) when compared with RMSEs of overall voyage. On average, the IMOS routine fluxes slightly overestimate heat fluxes as compared to CAPRICORN fluxes.

4.2 Assessment of ERA-Interim with ship and buoy fluxes

ERA-Interim 3-hourly fluxes are compared with CAPRICORN fluxes for March – April 2016 (figure 2) and with SOFS (figure 3) for March 2015 – April 2016. ERA-Interim estimates H_l with relative bias of less than 5%, but it overestimates H_s (>35% bias) when compared with buoy fluxes (table 1b). However, when compared with CAPRICORN fluxes, it performs worse for H_l (~10% relative bias) than H_s (~6% relative bias) as seen in table 1a. ERA-Interim also shows larger variance in fluxes when compared to CAPRICORN fluxes.

The product might perform very differently over different latitudes. Hence, to analyse this hypothesis, ERA-Interim 3-hourly fluxes are analysed for lower and higher latitudes. Here, the location of SOFS buoy at ~47°S is considered as the dividing line with >47°S is considered higher latitudes and vice versa. ERA-Interim gives positive bias (1.6 Wm^{-2}) and higher relative bias (8.3%) in H_s when ship is at lower latitudes (<47°S). But gives higher positive bias (14.4 Wm^{-2}) and higher relative bias (24.5%) in H_l when ship is at higher latitudes (>47°S). Overall, ERA-Interim gives higher uncertainty in H_s at lower latitudes as noted through the comparison with both ship and buoy fluxes whereas at higher latitudes, larger uncertainty is recorded in H_l. Further, ERA-Interim flux values are compared with CAPRICORN fluxes using mean error (or bias) statistic during pre-, midst- and post- cyclonic conditions during the traversal of 9 extratropical cyclones. ERA-Interim yields a higher positive bias in H_l (~12 Wm^{-2}) than in H_s (~10 Wm^{-2}) in the pre-frontal conditions. However, bias becomes negative for H_s (~-8.1 Wm^{-2}) and decreases for H_l (~4.9 Wm^{-2}) during mid-cyclone conditions. The bias again becomes positive for H_s (~0.5 Wm^{-2}) but continues to decrease for H_l (~-9.7 Wm^{-2}) in post-frontal conditions.

The product performance is also evaluated with respect to increasing wind speeds ranging from 1-20 ms^{-1} and for rain conditions with respect to both CAPRICORN and buoy fluxes. For buoy, the average rain rate was recorded as 0.02 mmh^{-1} for the given time-period. Low rain rate (<1 mmh^{-1}) was observed more than 60% of the time. Further, independent analyses of ERA-Interim with respect to the voyage and buoy reveals no systematic bias in ERA-Interim fluxes with respect to either wind speeds or rain rates.

4.3 Assessment of OAFlux with ship and buoy fluxes

The OAFlux data are available on a daily scale, so, the sample size is small (33 points) for the voyage. A strong positive correlation (~0.9, p-value close to zero) is found for both H_s and H_l when compared with CAPRICORN bulk fluxes. There is a better agreement (bias -0.3 Wm^{-2}) in H_s than in H_l (bias 9.3 Wm^{-2}) between OAFlux and CAPRICORN fluxes as seen in table 1a. The error statistics (table 1a) have been calculated after the grid-wise extraction of the daily flux data relative to the ship track. Further, for comparison purpose, ERA-Interim fluxes are extracted at 1° resolution on a daily time scale and are plotted alongside OAFlux fluxes as shown in figure 2e and 2f. ERA-Interim underestimates H_s (bias -0.66 Wm^{-2}) and overestimates H_l values (bias ~20 Wm^{-2}). Altogether, OAFlux performs better than ERA-Interim at the daily resolution.

When compared with buoy fluxes, OAFlux underestimates (bias ~-7 Wm^{-2}) H_l but gives near accurate estimates of H_s. Conclusively, OAFlux consistently gives a higher bias in H_l when compared with either ship or buoy fluxes. However, no conclusive systematic bias is observed in OAFlux values with respect to increasing wind speeds when compared with buoy data.

5. Discussion

We have compared the average performance of ERA-Interim, OAFlux and IMOS flux products over the Australian sector of the Southern Ocean with respect to bulk fluxes acquired using the NOAA PSD flux system during a month-long CAPRICORN experiment in March-April 2016 and the 13-month (2015-2016) SOFS data. The comparison is performed for lower latitudes (<47°S) based on both buoy and ship fluxes, and for higher latitudes (>47°S) based on ship fluxes with the location of the buoy at ~47 S as the dividing line.

The comparison reveals for ERA-Interim large positive bias in H_l (~14.43 Wm^{-2}) at higher latitudes and in H_s (~1.64 Wm^{-2}) at lower latitudes. A similar result was obtained by Brunke *et al.*, (2011) who observed that ERA-Interim performs better for H_l than for H_s in the tropics and mid-latitudes. In contrast to our results, Lindsay *et al.*, (2014) observed an underestimation in H_l but overestimation in H_s over the Arctic region (>65°N). Further, the RMSEs noted in ERA-Interim fluxes are relatively higher (~24 Wm^{-2} in H_s and ~43 Wm^{-2} in H_l)

at higher latitudes but lower (<20 Wm^{-2} for both fluxes) at lower latitudes over the analysis region as compared to the previous findings which estimated RMSEs in heat fluxes of the order ~20 Wm^{-2} over the land regions (Balsamo et al. 2015; Szczypta et al. 2011).

The daily OAFlux gives a higher bias in H_l as compared to H_s, which is very close (average within $\pm$ 0.5 Wm^{-2}) to the ship and buoy averages. It overestimates (bias 8.75 Wm^{-2}) H_l at higher latitudes but underestimates (bias -3.81 Wm^{-2}) at lower latitudes. However, the sample size is not significant (16 points) for high latitude regions. These findings are in agreement with previous results which observed OAFlux behaviour over the different oceans (Brunke et al. 2011; Santorelli 2011; Tomita et al. 2016). However, OAFlux gives larger bias in magnitude over the Southern Ocean region examined in our study as compared to the global oceans [0.04 Wm^{-2} for H_s and 0.98 Wm^{-2} for H_l respectively (Yu et al. 2008)].

All the bulk parameterization algorithms use equations (1) - (3) as the base, yet, the estimated turbulent fluxes differ either due to differences in the input bulk variables or the physical parameterizations used for various key processes. The desired accuracy of the mean (or bias) under nominal conditions has been determined to be within 0.2 ms^{-1} for wind speed, 0.2°C for air temperature, 0.1°C for sea surface temperature and 0.3 gkg^{-1} for specific humidity in order to attain ±10 Wm^{-2} accuracy in monthly surface net heat flux (Bradley and Fairall 2006; Weller et al. 2004). Tables 2a and 2b summarise these four input variables – air temperature (T_a), skin sea surface temperature (T_s), specific humidity (q) and 10-m wind speed (U_{10}) with respect to ship and buoy observations.

ERA-Interim has the highest uncertainties in T_a (bias -0.5 ms^{-1}) when compared with buoy observations, and in T_s (bias -0.4 °C) when compared with ship observations. However, ERA-Interim has lower bias in U_{10} but higher bias in T_s over this Southern Ocean region when compared with biases noted in the Drake Passage (Jiang et al. 2012). Further, ERA-Interim gives higher bias (in magnitude) in H_l than in H_s during pre and post-frontal conditions. This could be due to higher positive biases in U_{10} (bias 0.6 ms^{-1}) and q (bias 0.7 gkg^{-1}) during post-conditions. The mean bias in bulk variables improves during midst- conditions as compared to pre- and post- conditions. Overall, ERA-Interim performs better than OAFlux for fluxes as well as bulk variables as evident in figure 3.

IMOS routine ship observations are closest to NOAA PSD observations, however, IMOS underestimates T_a (mean error -0.2°C) and T_s (mean error -0.1°C), and overestimates U_{10} (mean error 0.4 ms^{-1}). OAFlux has high mean errors in T_a (0.9°C), q (0.4 gkg^{-1}) and T_s (0.4°C) when compared with ship observations. OAFlux underestimates (bias -0.4 ms^{-1}) U_{10} when compared with buoy observations but gives high overall RMSE of ~0.9 ms^{-1} over the analysis

region. Similar results were reported by Yu *et al.*, (2008) who attributed rain as a possible reason for the degradation of SSMI wind speed retrievals.

Figure 4 displays the comparison of monthly fluxes and bulk variables with SOFS buoy data for March 2015-April 2016 time-period along with the expected accuracy of mean. H_s by both products is not within $\pm$ 5 Wm^{-2} during February, March and November months. For H_l however, the products are only accurate to within $\pm$ 10 Wm^{-2} for all months except for February and March. ERA-Interim consistently underestimates T_a whereas both the products display highest uncertainties in T_s and U_{10}. Despite agreement for q at daily scale, the bias is low for mean monthly values for both the products and fall within the desired level of accuracy. Altogether, the level of accuracy is high for H_s and products perform better on average during the winter season (May-October).

The differences in the parameterizations of the bulk algorithms may also be accounted for the differences in the flux estimations. Since both IMOS routine observations and OAFlux evaluate fluxes using the COARE bulk algorithm, it comes down to the differences in the COARE and ECMWF algorithms. Brunke *et al.*, (2002) attributed surface wave spectrums, roughness length formulation, consideration of convective gustiness, salinity effect on ocean surface saturated humidity, and turbulent exchange coefficient formulation as major key differences in the parameterization schemes that contribute significantly to flux variations. Table 3 contrasts these formulations used in the COARE and ECMWF algorithms. Since these algorithms are based on the MOST theory, the parameterization of transfer coefficients follows the similar routine. Both the algorithms resort to similar parameterizations for salinity effect on ocean surface saturated humidity as well. The cool skin - warm layer diurnal effect in sea surface temperature is also incorporated in both the schemes using the same method (ECMWF 2015a; Fairall et al. 1996a). Despite these similarities, the most obvious difference is in the formulation of roughness lengths, which plays a major role in the formulation of transfer coefficients. The ECMWF calculates the wave-age dependent Charnock coefficient (Janssen 2008) whereas COARE 3.5 algorithm calculates the Charnock coefficient based on wind-speed dependent formulation (Edson et al. 2013) as shown in table 3 which implies a mature sea-state in balance with the wind forcing. In the present study, the Charnock coefficient from ECMWF is generally higher (~0.95 x 10^{-2} – ~6.44 x 10^{-2}) than observed values (1.1 x 10^{-2} – 1.8 x 10^{-2}) as the determining constant, $\hat{\alpha}$ is found by trial and error method (ECMWF 2015b). Further, thermal and moisture roughness lengths in ECMWF scheme are estimated to be higher by approximately 50-400% and 130-800%, respectively as compared to COARE 3.5 bulk values, for the given wind speeds during the R/V *Investigator* voyage. This could be one of the reasons for higher heat and moisture transfer coefficients in ECMWF scheme leading to overestimation in H_s and H_l. Further, in the COARE 3.5 algorithm, both the

thermal and moisture roughness length are equal whereas the moisture roughness length is estimated to be higher in ECMWF. It has been previously observed that COARE 3.5 wind speed dependent formulation without wave information agrees well with the observations (Edson et al. 2013). Edson, (2008) states a good agreement for the drag coefficient between COARE and ECMWF schemes despite these differences. Further, the comparison of wind speeds including gustiness during the voyage indicates a probable overestimation of wind gustiness by ECMWF as well.

6. Conclusion

We compared the surface heat fluxes obtained from ERA-Interim reanalysis and OAFlux hybrid data set with those measured during CAPRICORN experiment (with the NOAA PSD flux system and IMOS routine observations) carried out onboard *R/V Investigator* voyage (March – April 2016) and SOFS buoy deployed for a year (2015-2016) in the Australian sector of the Southern Ocean. With the current aim to reconcile surface flux accuracy to within 5 Wm^{-2} at 3-6 hour resolution, overall, ERA-Interim (3-hourly at 0.25°) and OAFlux (daily at 1°) estimate sensible heat flux, H_s accurate to ± 5 Wm^{-2}, but not latent heat flux, H_l. ERA-Interim gives a higher bias in H_s at lower latitudes (<47°S) and in H_l at higher latitudes (>47°S). Similarly, OAFlux provides good estimates of H_s (bias within ± 0.5 Wm^{-2}) but consistently gives higher bias (within ± 10 Wm^{-2}) in H_l across the range of latitudes sampled (44°S - 53°S). The biases in ERA-Interim heat flux estimates can be attributed to higher bias in T_a and U_{10} at lower latitudes, and in T_s at higher latitudes. Whereas OAFlux has high uncertainty in U_{10} at lower latitudes but in T_a and T_s at higher latitudes.

Other than uncertainties in bulk variables, the ECMWF scheme overestimates roughness lengths and wind gustiness which might explain the overestimation in heat fluxes. While OAFlux has been noted to agree well with ship-based climatology at seasonal and annual time scale (Yu et al. 2008), the current analysis shows that it can also be used at daily time scale for lower latitudes for the study of heat fluxes and energy budget. However, its application in studying mesoscale systems remains limited due to its coarse spatiotemporal resolution. IMOS routine ship observations overestimate H_s (~11%) and H_l (~3%) as compared to the NOAA PSD flux observations during the voyage. But since these are observations, they are closest to what was observed by the NOAA PSD system during *R/V Investigator* voyage. Conclusively, there is still a need to quantify the uncertainty in measurements and derived fluxes under extreme conditions.

Acknowledgement

This research is supported by the ARC Centre of Excellence for Climate System Science (grant DP150102894). Authors are thankful to the CSIRO Marine National Facility (MNF) for its grant of sea time on *R/V Investigator* and associated personnel, scientific equipment, and data management. The first author extends the appreciation for the ECMWF support team, Paul Berrisford and Anton Beljaars for their help. Finally, we would like to acknowledge the crucial roles played by Tom Trull (CSIRO), the lead chief scientist, Tegan Sime, the MNF voyage manager, and the *Investigator* cooks to make this research voyage a success.

References

Balsamo, G., and Coauthors, 2015: ERA-Interim/Land: A global land surface reanalysis data set. *Hydrology and Earth System Sciences*, **19**, 389–407, doi:10.5194/hess-19-389-2015.

Bariteau, L., C. Fairall, B. Blomquist, and S. Pezoa, 2018: CAPRICORN 2016 Field campaign: surface meteorological data and turbulent fluxes collected from the RV Investigator by the National Oceanographic and Atmospheric Administration (NOAA) in the Indian and South Pacific Oceans from 2016-03-14 to 2016-04-15 (NC. doi:10.7289/V5Q81BBC.

Beljaars, A. C. M., 1998: Air-sea interaction in the ECMWF model. *Seminar on Atmosphere-surface Interaction, 8-12 September 1997*, Shinfield Park, Reading.

Bharti, V., B. W. Blomquist, C. W. Fairall, Y. Huang, A. Protat, P. P. Sullivan, S. T. Siems, and M. J. Manton, 2018: Air-sea heat and momentum fluxes in the Southern Ocean. *Journal of Geographical Research: Atmospheres*,.

Bôas, A. B. V., O. T. Sato, A. Chaigneau, and G. P. Castelão, 2015: The signature of mesoscale eddies on the air-sea turbulent heat fluxes in the South Atlantic Ocean. *Geophysical Research Letters*, **42**, 1856–1862, doi:10.1002/2015GL063105.1.

Bourassa, M. A., and Coauthors, 2013: High-latitude ocean and sea ice surface fluxes: Challenges for climate research. *Bulletin of the American Meteorological Society*, **94**, 403–423, doi:10.1175/BAMS-D-11-00244.1.

Bradley, F., and C. Fairall, 2006: A guide to making climate quality meteorological and flux measurements at sea. *NOAA Technical Memorandum*, **OAR PSD-31**.

Brunke, M. A., X. Zeng, and S. Anderson, 2002: Uncertainties in sea surface turbulent flux algorithms and data sets. *Journal of Geophysical Research*, **107**, 3141, doi:10.1029/2001JC000992.

——, C. W. Fairall, X. Zeng, L. Eymard, and J. A. Curry, 2003: Which Bulk Aerodynamic Algorithms are Least Problematic in Computing Ocean Surface Turbulent Fluxes? *Journal of Climate*, **16**, 619–635, doi:10.1175/1520-0442(2003)016<0619:WBAAAL>2.0.CO;2. http://journals.ametsoc.org/doi/abs/10.1175/1520-0442%282003%29016%3C0619%3AWBAAAL%3E2.0.CO%3B2.

——, Z. Wang, X. Zeng, M. Bosilovich, and C. L. Shie, 2011: An assessment of the uncertainties in ocean surface turbulent fluxes in 11 reanalysis, satellite-derived, and combined global datasets. *Journal of*

Climate, **24**, 5469–5493, doi:10.1175/2011JCLI4223.1.

Chou, S. H., E. Nelkin, J. Ardizzone, R. M. Atlas, and C. L. Shie, 2003: Surface turbulent heat and momentum fluxes over global oceans based on the goddard satellite retrievals, version 2 (GSSTF2). *Journal of Climate*, **16**, 3256–3273, doi:10.1175/1520-0442(2003)016<3256:STHAMF>2.0.CO;2.

Curry, J. A., and Coauthors, 2004: Seaflux. *Bulletin of the American Meteorological Society*, **85**, 409–424, doi:10.1175/BAMS-85-3-409. http://journals.ametsoc.org/doi/abs/10.1175/BAMS-85-3-409.

Decker, M., M. A. Brunke, Z. Wang, K. Sakaguchi, X. Zeng, and M. G. Bosilovich, 2012: Evaluation of the reanalysis products from GSFC, NCEP, and ECMWF using flux tower observations. *Journal of Climate*, **25**, 1916–1944, doi:10.1175/JCLI-D-11-00004.1.

Dee, D. P., and Coauthors, 2011: The ERA-Interim reanalysis: Configuration and performance of the data assimilation system. *Quarterly Journal of the Royal Meteorological Society*, **137**, 553–597, doi:10.1002/qj.828.

Dong, S., S. T. Gille, and J. Sprintall, 2007: An assessment of the Southern Ocean mixed layer heat budget. *Journal of Climate*, **20**, 4425–4442, doi:10.1175/JCLI4259.1.

ECMWF, 2015a: *IFS DOCUMENTATION – Cy41r Operational implementation 12 May 2015 Part IV: Physical Processes*. 1-210 pp.

——, 2015b: *IFS DOCUMENTATION – Cy41r1 Operational implementation 12 May 2015 Part VII : ECMWF Wave Model*. 1-83 pp.

Edson, J. B., 2008: Review of Air-Sea Transfer Processes. *ECMWF Workshop on Ocean-Atmosphere Interactions*, 10–12.

——, 2015: Improved Parameterization of Heat, Mass and Momentum Exchange for Process Studies in Numerical Models. 15–16.

Edson, J. B., and Coauthors, 2013: On the Exchange of Momentum over the Open Ocean. *Journal of Physical Oceanography*, **43**, 1589–1610, doi:10.1175/JPO-D-12-0173.1.

Fairall, C. W., E. F. Bradley, J. S. Godfrey, G. a Wick, J. B. Edson, and G. S. Young, 1996a: Cool-skin and warm-layer effects on sea surface temperature. *J. Geophys. Res.*, **101**, 1295–1308, doi:10.1029/95jc03190. http://dx.doi.org/10.1029/95JC03190.

——, ——, D. P. Rogers, J. B. Edson, and G. S. Young, 1996b: Bulk parameterization of air-sea fluxes for Tropical Ocean-Global Atmosphere Coupled-Ocean Atmosphere Response Experiment. *Journal of Geophysical Research*, **101**, 3747, doi:10.1029/95JC03205.

Fairall, C. W., E. F. Bradley, J. E. Hare, A. A. Grachev, and J. B. Edson, 2003: Bulk parameterization of air-sea fluxes: Updates and verification for the COARE algorithm. *Journal of Climate*, **16**, 571–591, doi:10.1175/1520-0442(2003)016<0571:BPOASF>2.0.CO;2.

Fairall, C. W., and Coauthors, 2010: Observations to Quantify Air-Sea Fluxes and Their Role in Climate Variability and Predictability. *Proceedings of OceanObs'09: Sustained Ocean Observations and Information for Society, Vol. 2.*, 299–313, doi:10.5270/OceanObs09.cwp.27. https://abstracts.congrex.com/scripts/jmevent/abstracts/FCXNL-09A02a-1664389-1-cwp2b03.pdf%5Cnhttp://eprints.soton.ac.uk/71643/.

Fasullo, J. T., and K. E. Trenberth, 2008: The annual cycle of the energy budget. Part I: Global mean and

land-ocean exchanges. *Journal of Climate*, **21**, 2297–2312, doi:10.1175/2007JCLI1935.1.

Frenger, I., N. Gruber, R. Knutti, and M. Münnich, 2013: Imprint of Southern Ocean eddies on winds, clouds and rainfall. *Nature Geoscience*, **6**, 608–612, doi:10.1038/ngeo1863. http://www.nature.com/doifinder/10.1038/ngeo1863.

Gille, S., M. A. Bourassa, and C. A. Clayson, 2010: Improving observations of high-latitude fluxes between atmosphere, ocean, and ice. *Eos*, **91**, 307, doi:10.1029/2010EO350003.

Herman, A., 2015: Trends and variability of the atmosphere–ocean turbulent heat flux in the extratropical Southern Hemisphere. *Scientific Reports*, **5**, doi:10.1038/srep14900. http://www.nature.com/articles/srep14900.

Janssen, P. A. E. M., 2008: Air-sea interaction through waves. *ECMWF Workshop Workshop on Ocean-Atmosphere Interactions*, 10–12.

Jiang, C., S. T. Gille, J. Sprintall, K. Yoshimura, and M. Kanamitsu, 2012: Spatial variation in turbulent heat fluxes in Drake Passage. *Journal of Climate*, **25**, 1470–1488, doi:10.1175/2011JCLI4071.1.

Josey, S. A., E. C. Kent, and P. K. Taylor, 1999: New insights into the ocean heat budget closure problem from analysis of the SOC air-sea flux climatology. *Journal of Climate*, **12**, 2856–2880, doi:10.1175/1520-0442(1999)012<2856:NIITOH>2.0.CO;2.

Lindsay, R., M. Wensnahan, A. Schweiger, and J. Zhang, 2014: Evaluation of seven different atmospheric reanalysis products in the arctic. *Journal of Climate*, **27**, 2588–2606, doi:10.1175/JCLI-D-13-00014.

Liu, J., T. Xiao, and L. Chen, 2011: Intercomparisons of air-sea heat fluxes over the Southern Ocean. *Journal of Climate*, **24**, 1198–1211, doi:10.1175/2010JCLI3699.1.

Reynolds, R. W., T. M. Smith, C. Liu, D. B. Chelton, K. S. Casey, and M. G. Schlax, 2007: Daily high-resolution-blended analyses for sea surface temperature. *Journal of Climate*, **20**, 5473–5496, doi:10.1175/2007JCLI1824.1.

Santorelli, A., 2011: Differences between two estimates of air-sea turbulent heat fluxes.pdf. *Journal of Geophysical Research*, **116**.

Schulz, E. W., M. A. Grosenbaugh, L. Pender, D. J. M. Greenslade, and T. W. Trull, 2011: Mooring design using wave-state estimate from the Southern Ocean. *Journal of Atmospheric and Oceanic Technology*, **28**, 1351–1360, doi:10.1175/JTECH-D-10-05033.1.

——, S. A. Josey, and R. Verein, 2012: First air-sea flux mooring measurements in the Southern Ocean. *Geophysical Research Letters*, **39**, 1–9, doi:10.1029/2012GL052290.

Szczypta, C., J. C. Calvet, C. Albergel, G. Balsamo, S. Boussetta, D. Carrer, S. Lafont, and C. Meurey, 2011: Verification of the new ECMWF ERA-Interim reanalysis over France. *Hydrology and Earth System Sciences*, **15**, 647–666, doi:10.5194/hess-15-647-2011.

Tomita, H., T. Senjyu, and M. Kubota, 2016: Evaluation of air-sea sensible and latent heat fluxes over the Japan Sea obtained from satellite, atmospheric reanalysis, and objective analysis products. *Journal of Oceanography*, doi:10.1007/s10872-016-0368-y. http://link.springer.com/10.1007/s10872-016-0368-y.

Trenberth, K. E., and J. T. Fasullo, 2010: Tracking Earth's Energy. *climate change*, **328**, 316–318.

Weller, R. A., F. Bradley, and R. Lukas, 2004: The interface or air-sea flux component of the TOGA coupled ocean-atmosphere response experiment and its impact on subsequent air-sea interaction studies. *Journal of Atmospheric and Oceanic Technology*, **21**, 223–257, doi:10.1175/1520-0426(2004)021<0223:TIOAFC>2.0.CO;2.

Yu, L., and R. A. Weller, 2007: Objectively analyzed air-sea heat fluxes for the global ice- free oceans (1981-2005). *Bulletin of the American Meteorological Society*, **88**, 527–539, doi:10.1175/BAMS-88-4-527.

——, ——, and B. Sun, 2004: Mean and variability of the WHOI daily latent and sensible heat fluxes at In situ flux measurement sites in the Atlantic Ocean. *Journal of Climate*, **17**, 2096–2118, doi:10.1175/1520-0442(2004)017<2096:MAVOTW>2.0.CO;2.

——, X. Jin, and R. a. Weller, 2007: Annual, Seasonal, and Interannual Variability of Air–Sea Heat Fluxes in the Indian Ocean. *Journal of Climate*, **20**, 3190–3209, doi:10.1175/JCLI4163.1.

Yu, L., X. Jin, and R. A. Weller, 2008: *Multidecade Global Flux Datasets from the Objectively Analyzed Air-sea Fluxes (OAFlux) Project: Latent and Sensible Heat Fluxes, Ocean Evaporation, and Related Surface Meteorological Variables*. 64 pp.

Yu, L., Z. Zhang, S. Zhong, M. Zhou, Z. Gao, H. Wu, and B. Sun, 2011: An inter-comparison of six latent and sensible heat flux products over the southern ocean. *Polar Research*, **30**, 1–27, doi:10.3402/polar.v30i0.10167.

Table 1a: Error statistics for H_s and H_l at given time-scales for *R/V Investigator* voyage. CAPRICORN bulk fluxes are extracted for the given products and their respective time periods. Missing values are excluded prior to comparison. The fluxes are defined as positive upwards. The unit is Wm^{-2} for all statistics except for the percent bias.

	Hourly (24/03/2016-15/04/2016)		**3-hourly (14/03/2016 – 15/04/2016)**		**Daily (14/03/2016 – 15/04/2016)**	
	H_s	***H_l***	***H_s***	***H_l***	***H_s***	***H_l***
CAPRICORN flux mean	17.76	81.50	16.59	75.83	16.77	76.94
Product mean*	19.84	83.78	17.56	83.12	16.44	86.23
CAPRICORN flux standard deviation or σ	29.99	65.09	32.15	72.50	26.73	63.37
Product σ*	30.40	68.62	41.48	77.85	30.35	67.86
Mean error or bias	2.07	2.27	0.97	7.29	-0.32	9.28
Relative bias or percent bias (%)	11.7	2.79	5.88	9.61	-1.95	12.07
Root mean square error or RMSE	9.06	19.23	24.07	42.90	12.94	33.54

*hourly product – IMOS, 3-hourly product – ERA-Interim, daily product – OAFlux

Table 1b: Error statistics for H_s and H_l for SOFS buoy, ERA-Interim and OAFlux products at daily time scale. All units in Wm^{-2} except for the percent bias.

	SOFS Buoy		**ERA-Interim**		**OAFlux**	
	H_s	***H_l***	***H_s***	***H_l***	***H_s***	***H_l***
Mean	9.18	64.04	12.41	65.98	9.261	59.59
σ	25.37	53.71	27.10	52.63	24.10	40.22
Mean error or bias			3.23	1.93	0.076	-4.44
Relative bias or percent bias (%)			35.19	3.02	0.083	-6.94
RMSE			10.31	16.40	9.92	22.07

Table 2a: Mean and standard deviation of air temperature (T_{air}), sea surface temperature (T_s), specific humidity (q) and 10-m wind speed (U_{10}) for the given datasets on the given spatiotemporal scales during *R/V Investigator*.

	Hourly CAPRICORN flux data	Hourly IMOS	3-hourly CAPRICORN flux	3-hourly ERA-Interim	Daily CAPRICORN flux	Daily OAFlux
T_a (°C)	9.23±2.90	9.05±2.86	10.19±2.94	10.18±2.87	10.24±2.73	11.14±2.60
T_s (°C)	10.63±3.25	10.54±3.21	11.57±3.26	11.16±2.92	11.63±3.14	12.07±2.88
q (g kg^{-1})	5.68±1.40	5.69±1.48	6.20±1.64	6.30±1.52	6.20±1.39	6.65±1.04
U_{10} (ms^{-1})	11.59±3.51	11.99±3.52	10.52±3.74	10.76±3.76	10.54±3.06	10.41±3.30

Table 2b: Mean and standard deviation of air temperature (T_{air}), sea surface temperature (SST), specific humidity (q) and 10-m wind speed (U_{10}) for the given datasets as compared to SOFS Buoy on a daily time scale.

	SOFS Buoy	ERA-Interim	OAFlux
T_a (°C)	9.89±1.82	9.38±2.0	9.77±1.82
T_s (°C)	10.39±1.36	10.14±1.20	10.30±1.07
q (g kg^{-1})	6.13±1.17	6.00±1.28	6.17±0.96
U_{10} (ms^{-1})	9.31±2.97	10.09±3.78	10.03±3.22

Table 3: formulations used in COARE 3.0/3.5 bulk model and ECMWF scheme for the five contributing factors in the parameterizations

Physical parameterization	COARE 3.0/3.5 model	ECMWF scheme
Surface wave spectrum	*Does not use coupled wave model* *To model the effect of sea state and wave age,* $\frac{z_0^{rough}}{\gamma} = D\left(\frac{u_*}{C_p}\right)^2$ z_0^{rough} *roughness length for rough flow* γ *significant wave height* u_* *friction velocity* C_p *phase speed of dominant*	$\frac{d}{dt}F = S = S_{in} + S_{nl} + S_{diss}$ S_{in} *generation of waves by wind* S_{nl} *nonlinear four-wave interaction* S_{diss} *dissipation of ocean waves e.g wave breaking*

	$\frac{u_*}{C_p}$ *inverse wave age*	
Roughness length formulation	*velocity roughness length* = $z_{OM} = \alpha_M \frac{\nu}{u_*} + \alpha_{Ch} \frac{u_*^2}{g}$ *thermal roughness length* $z_{OH} = \alpha_H \frac{\nu}{u_*}$ *moisture roughness length* $z_{OQ} = \alpha_Q \frac{\nu}{u_*}$ *Charnock coefficient* α_{Ch} $= \begin{cases} 0.011 for S \leq 10 ms^{-1} \\ 0.011 + \frac{0.007}{8}(S-10) for 10 < S \leq 18 \\ 0.018 for S \geq 18 ms^{-1} \end{cases}$ *S – mean wind speed w.r.t. ocean* $\alpha_M = 0.11$ $z_{OQ} = min(1.1 \times 10^{-4}, 5.5 \times 10^{-5} R_r^{-0.6})$ *Where* R_r *is roughness Reynolds number* $z_{OH} = z_{OQ}$	*Same roughness lengths equations as in COARE 3.5 but* $\alpha_{Ch} = 0.018$ *uncoupled model* $\alpha_{Ch} = \frac{\alpha}{\sqrt{1-\frac{\tau_w}{\tau}}}$ *coupled model (wave model) where* τ_w *wave-induced stress and* τ *is total stress* $\alpha_M = 0.11$ $\alpha_H = 0.40$ $\alpha_Q = 0.62$ *kinematic viscosity,* $\nu = 1.5 \times 10^{-5} m^2 s^{-1}$
Consideration of convective gustiness	$U_g = \beta W_* = \beta \left(\frac{g}{T} w' \theta_v' z_i\right)^{\frac{1}{3}}$ $W_* -$ *convective velocity scale* *z – depth of the convective boundary layer* U_g *– gustiness* $\beta = 1.25$	*Same equation as in COARE 3.5 but* $\beta = 1$
Salinity effect on ocean surface saturated humidity	$q_s = 0.98 q_{sat}(T_s)$ q_s *– water vapor mixing ratio* q_{sat} *– saturation mixing ratio* T_s *–sea surface temperature*	*Same as in COARE*
Turbulent exchange coefficient formulation	*total transfer coefficient* $C_x = c_x^{1/2} c_d^{1/2}$ *x can be u,v wind components, potential temperature,* θ *or water vapor specific humidity, q* c_x *– bulk transfer coefficient, d being used for wind speed* $c_x^{\frac{1}{2}}(\xi) = \frac{c_{xn}^{\frac{1}{2}}}{1 - \left(\frac{c_{xn}^{\frac{1}{2}}}{\kappa}\right)\psi_x(\xi)}$ $c_{xn}^{1/2} = \frac{\kappa}{ln\left(\frac{z}{z_{0x}}\right)}$ ξ*– MOST stability parameter, subscript n refers to neutral (*ζ *= 0) stability* ψ_x *– empirical function describing stability dependence of the mean profile* z_{0x} *-roughness length for x* κ*– von Kármán's constant*	*Same as in COARE*

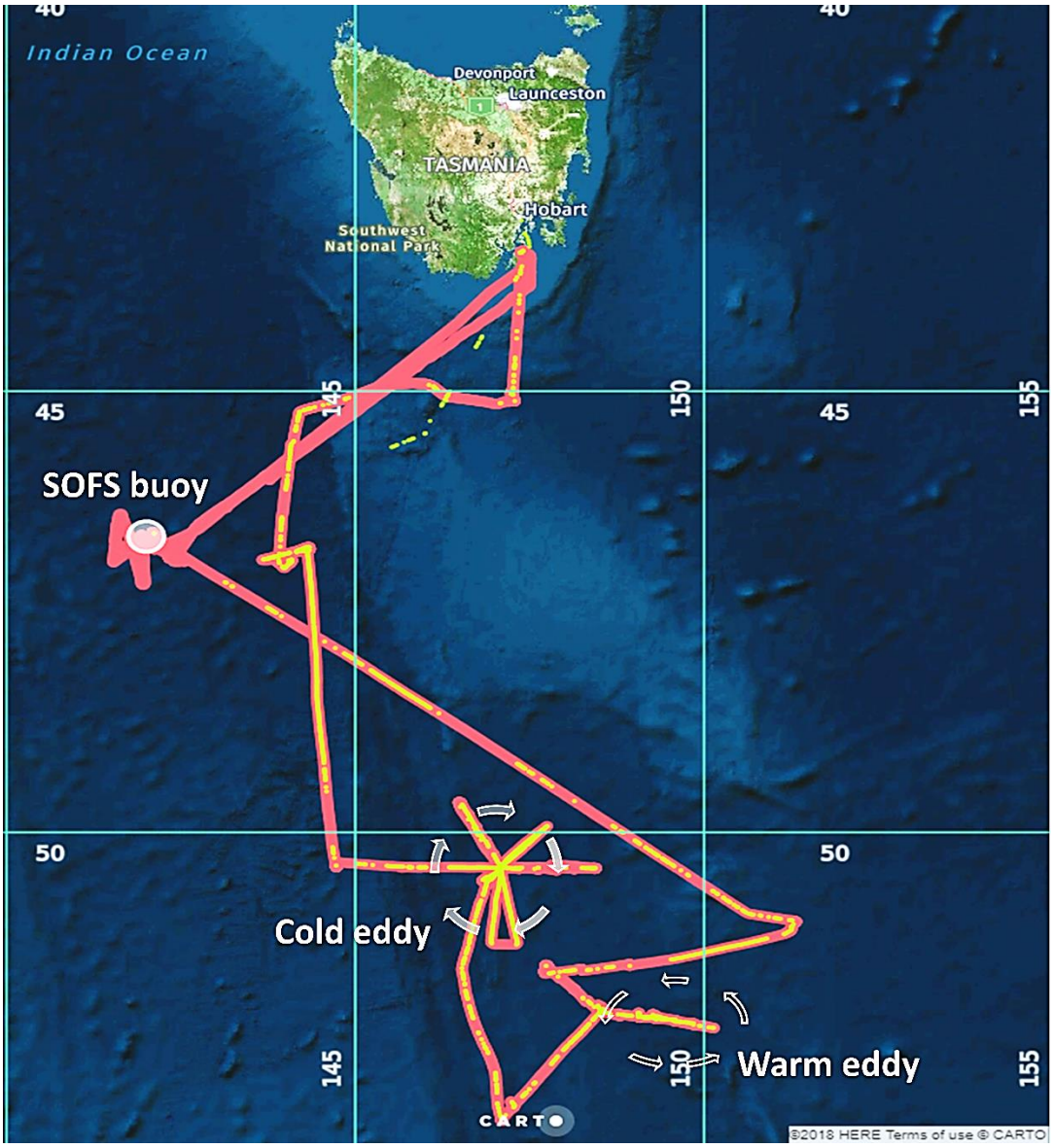
Indian Ocean
Devonport
Launceston
TASMANIA
Hobart
Southwest
National Park
40
45
50
145
150
155
SOFS buoy
Cold eddy
Warm eddy
CARTO
©2018 HERE Terms of use © CARTO

Figure 1: *R/V Investigator* cruise track in March-April 2016 with highlighted data availability of IMOS routine observations (yellow) as compared to COARE 3.5 bulk measurements (red). The location of SOFS buoy (~46.7°S 142°E) is shown with a circle.

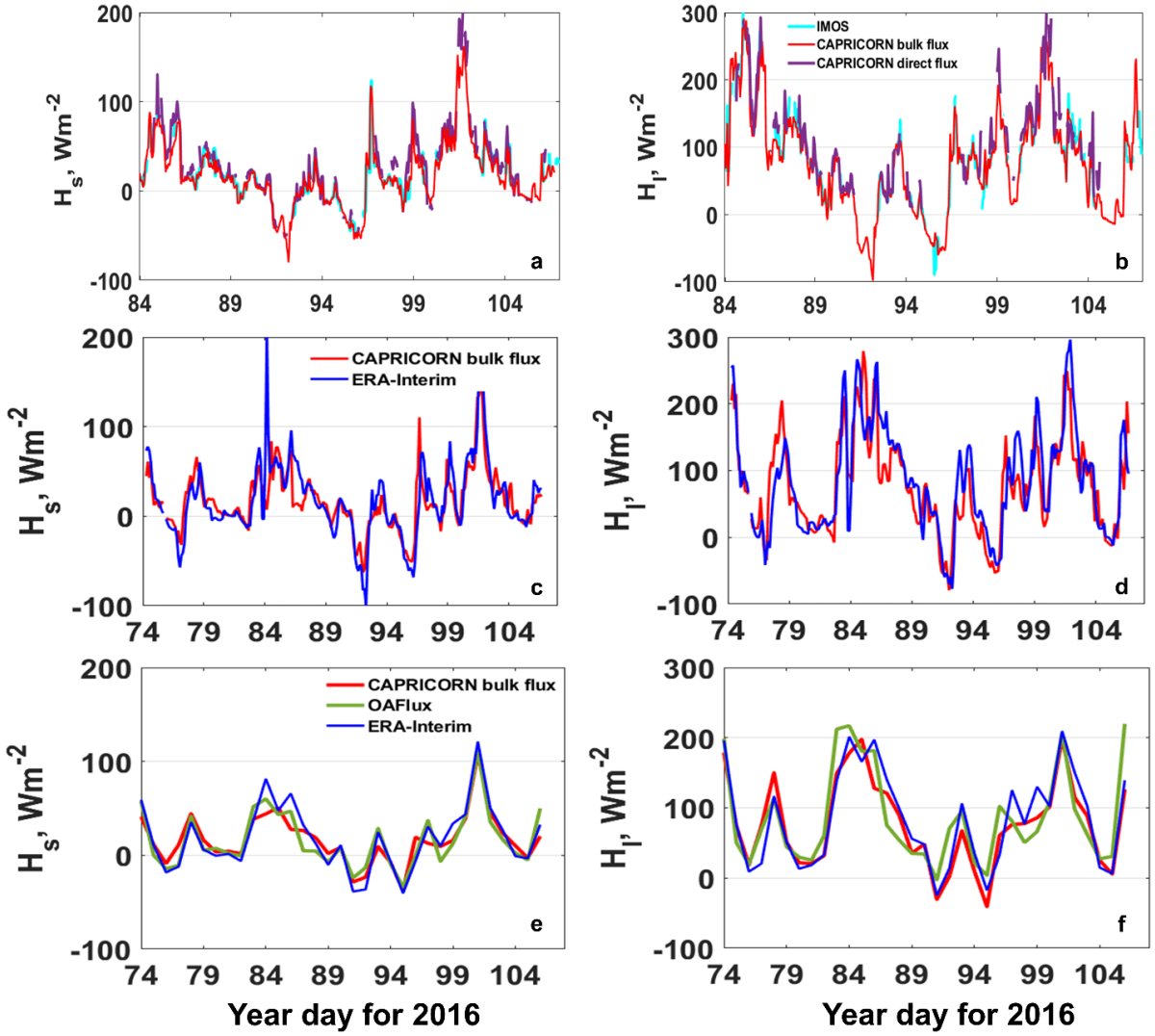

Figure 2: Comparison of time series of COARE 3.5 bulk fluxes at daily scale with OAFlux for (a) Sensible heat flux, H_s (b) Latent heat flux, H_l (c&d) same as a&b but with ERA-Interim at 3-hourly scale; (e&f) same as a&b but with IMOS routine observations at hourly scale during *R/V Investigator* voyage in March-April 2016.

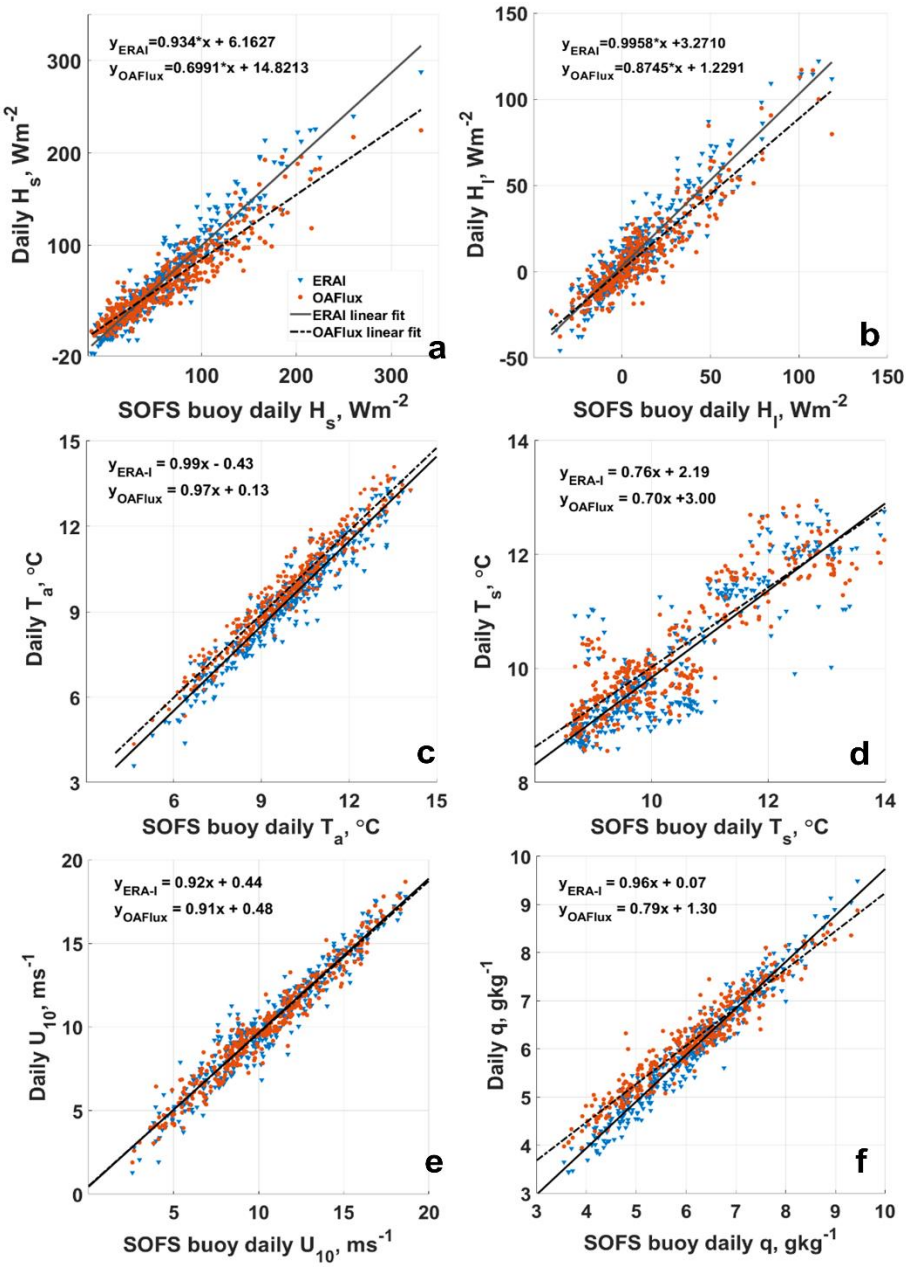

Figure 3: Scatterplots of daily ERA-Interim, OAFlux products with SOFS buoy data for (a) sensible heat flux, H_s (b) latent heat flux, H_l (c) air temperature, T_a (d) sea surface temperature, T_s (e) specific humidity, q (f) wind speed, U_{10} for the year 2015-2016.

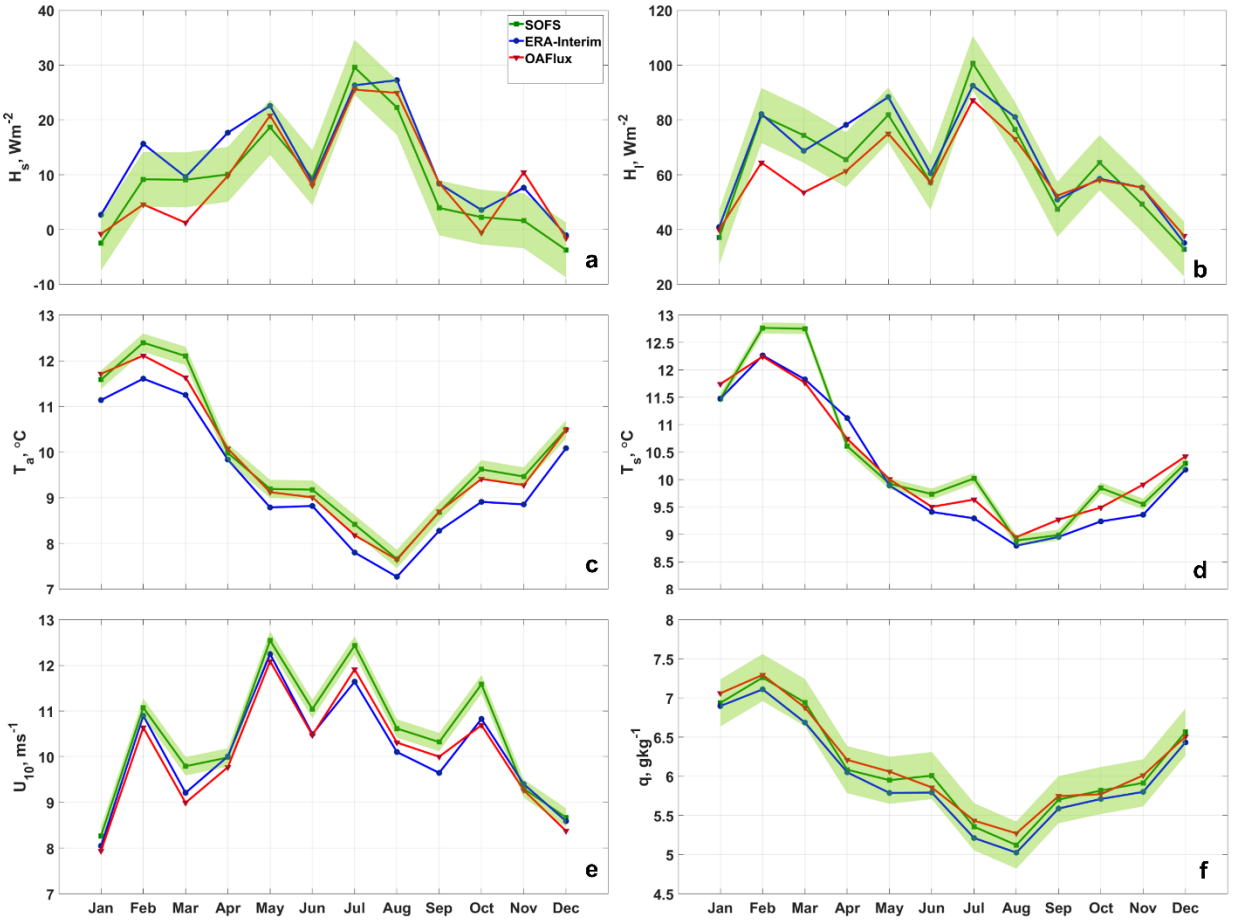

Figure 4: Mean monthly variation displayed along with target accuracy of mean as shaded area obtained by SOFS buoy, OAFlux and ERA-Interim products for (a) sensible heat flux, H_s, $\pm$5 Wm^{-2} (b) latent heat flux, H_l $\pm$10 Wm^{-2} (c) air temperature, T_a $\pm$0.2 °C (d) 10-m wind speed, U_{10} $\pm$0.2 ms^{-1} (e) sea surface temperature, T_s $\pm$0.1 °C (f) specific humidity, q $\pm$0.3 gkg^{-1} for year 2015-2016.